

# Synthesis and Environmental Stability Analysis of $\text{Cu}_n\text{Co}_{1-n}$ -MOF-74 with Different Doping Ratios of Metal Ions

Fangshi Liu

**Abstract**—Metal-organic framework materials MOFs are porous crystalline materials with periodic framework structures composed of metal or metal oxide clusters and organic ligands, which are widely used in catalysis, energy storage (and separation). MOF-74 materials have a high density of potentially open metal sites in the backbone that can replace metal nodes without disrupting the basic backbone structure of MOF crystals, which makes the design of stable bimetallic/polymetallic MOF topologies are promising. The addition of two or more metal ions can add different metal properties to achieve more complex multiple catalysis, and it is important to develop and prepare new bimetallic MOFs materials. In this paper, five  $\text{Cu}_n\text{Co}_{1-n}$ -MOF-74 materials were successfully synthesized by a more stable classical solvothermal method using  $\text{Cu}^{2+}$  and  $\text{Co}^{2+}$  as bimetallic central ions and adjusting the doping ratio of  $\text{Co}^{2+}$  to  $\text{Cu}^{2+}$  in MOF-74 materials by controlling the ratio of metal raw materials. The five synthesized materials were characterized by XRD, IR, and RAMAN, and the metal distribution on the surface of the materials was observed by using EDS energy spectrometry instrument. Their environmental stability was also analyzed by ICP.

**Index Terms**—MOF-74; EDS; Synthesis; Environmental stability.

## I. INTRODUCTION

Metal-organic framework materials (MOF) are organic ligand coordination networks containing potential voids made of inorganic and organic units connected by strong chemical bonds based on the coordination of metal nodes or metal oxide clusters with organic linkers [1]. In simple terms, metal ions or clusters and organic ligands are combined to form spatial 3D structures. The pore structure and properties can be modified using the inherent properties of the metal ions as well as the ligands [2]. One study proposed a bimetallic MOF combination therapy strategy loaded with DNA enzymes, in order to effectively reduce the damage of chemotherapy on normal tissues and inhibit tumor recurrence and metastasis, which not only enables in vivo synthesis of antitumor drugs and avoids the side effects of conventional chemotherapy, but also DNA enzyme-mediated self-administered gene therapy can inhibit tumor metastasis, providing a new idea to improve the therapeutic effect [3].

MOF-74 materials consist of 11 Å one-dimensional hexagonal channels with high porosity, great surface area (SBET) and extremely high structural flexibility [4], and given these advantages, MOF-74 has been used in gas adsorption and separation [5], catalysis [6], sensing and biomedical [7] applications. Metal ion doping can modulate the electronic structure and enhance synergistic interactions, thus improving the material chemistry.

Fangshi Liu, College of Chemical and Environment Protection, Southwest Minzu University, Chengdu, China

While most MOFs contain only a single metal in the secondary structure unit, MOF-74 has a unique infinite secondary structure unit, which makes MOF-74 more tolerant to different metals in the single lattice system and can allow multiple metals to coexist in the secondary structure. The study by Chen successfully demonstrated the great potential of a series of homocrystalline bimetallic MOFs in catalytic  $\text{O}_3$  decomposition [8].

Currently, there are two main approaches for the synthesis of bimetallic nodal MOFs materials: (1) direct synthesis method, in which a hydrothermal method is used to influence the synthesis of bimetallic MOFs materials by controlling the amount of metal ion input; (2) post-synthetic modification method, in which the original part of metal ions in the backbone is replaced by ion exchange while keeping the MOF framework structure unchanged [9]. In this paper, we chose MOF-74 as the research object and prepared four  $\text{CuCo}$ -MOF-74 materials with different ion doping ratios by controlling the molar ratio of  $\text{Cu}^{2+}$  to  $\text{Co}^{2+}$ . The physical and chemical properties of the materials were also characterized.

## II. EXPERIMENTAL

### Materials preparation

The 2,5-dihydroxyterephthalic acid (99%), copper nitrate trihydrate (99%), cobalt nitrate hexahydrate (99%), N,N-dimethylformamide (DMF), and methanol used in the study were of analytical grade. The literature solvent thermal method was modified to synthesize  $\text{Cu}_n\text{Co}_{1-n}$ -MOF-74 materials with different ion doping ratios [8].

### Synthesis of Materials

As an example of the preparation method of  $\text{Cu}_{0.5}\text{Co}_{0.5}$ -MOF-74, 0.299 g of 2,5-dihydroxyterephthalic acid (dhtp) yellow powder was weighed with 54 mL of a mixture of N,N-dimethylformamide (DMF) and 6 mL of methanol, stirred well, and then 0.3658 g of  $\text{Cu}(\text{NO}_3)_2 \cdot 3\text{H}_2\text{O}$  blue solid was weighed with 0.4406 g of  $\text{Co}(\text{NO}_3)_2 \cdot 6\text{H}_2\text{O}$  pink solid into which the above solution was stirred until clarified, transferred into a 100 mL hydrothermal reaction kettle lined with PTFE, and reacted at 120 °C for 24 h. After the reaction was finished, it was cooled and taken out, filtered and centrifuged to collect the solid, and the solid product was washed three times with 20 mL DMF and twice with 20 mL methanol, filtered to separate the red-brown product, placed in drying under vacuum for 12 h at 50 °C,  $\text{Cu}_n\text{Co}_{1-n}$ -MOF-74 powder was obtained. The preparation of other doping ratios of  $\text{Cu}_n\text{Co}_{1-n}$ -MOF-74 is detailed in Table 1.

Table 1 Details of  $\text{Cu}_n\text{Co}_{1-n}\text{-MOF-74}$  material preparation

	dhtp /g	$\text{Cu}(\text{NO}_3)_2 \cdot 3\text{H}_2\text{O}$ /g	$\text{Co}(\text{NO}_3)_2 \cdot 6\text{H}_2\text{O}$ /g	Time /h
$\text{Cu}_{0.8}\text{Co}_{0.2}\text{-MOF-74}$	0.299	0.5852	0.1762	24
$\text{Cu}_{0.5}\text{Co}_{0.5}\text{-MOF-74}$	0.299	0.3658	0.4406	24
$\text{Cu}_{0.2}\text{Co}_{0.8}\text{-MOF-74}$	0.299	0.1463	0.7048	24

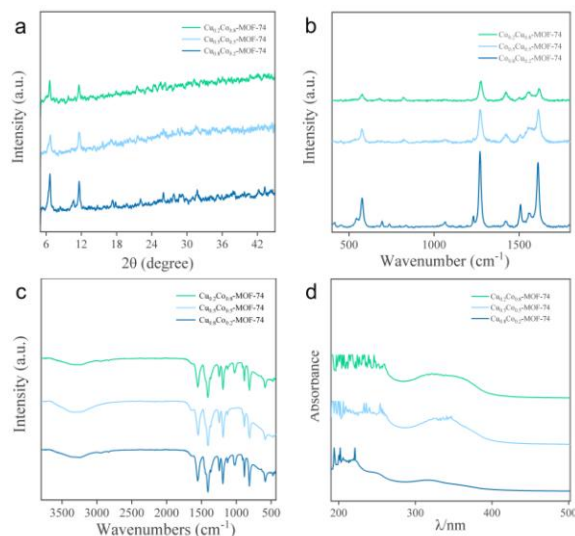
### III. RESULTS AND DISCUSSION

#### Characterization of $\text{Cu}_n\text{Co}_{1-n}\text{-MOF-74}$

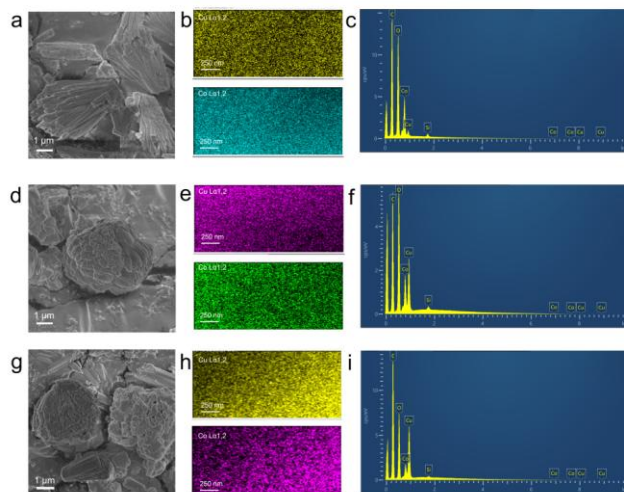
Three bimetallic MOF-74 sample powders were prepared showing what colors, as shown in Figure 1, are consistent with the literature reports [10]. The properties and crystal structures of the synthesized products were characterized by X-ray diffraction technique (XRD). All three  $\text{Cu}_n\text{Co}_{1-n}\text{-MOF-74}$  samples showed strong characteristic peaks at  $6.8 \text{ \AA}$  versus  $11.6 \text{ \AA}$  with good intensity of the exiting peaks and high crystalline phase content (Figure 2a), which is consistent with the XRD diffraction patterns of  $\text{Cu}_n\text{Co}_{1-n}\text{-MOF-74}$  reported in the literature [11].


 Figure 1 Morphology of the  $\text{Cu}_n\text{Co}_{1-n}\text{-MOF-74}$  materials.

The functional groups of the  $\text{Cu}_n\text{Co}_{1-n}\text{-MOF-74}$  were subjected to FTIR spectroscopy in the wavelength range of  $4000 \text{ cm}^{-1}$  to  $400 \text{ cm}^{-1}$ , and the results are shown in Figure 2b. The three samples showed meaningful peaks at  $1366 \text{ cm}^{-1}$ ,  $1448 \text{ cm}^{-1}$  and  $1644 \text{ cm}^{-1}$ , which could correspond to C-O stretching, C=O stretching and O-H bending vibrations of free carboxyl groups [12]. The changes in the structure of the molecular vibrational energy levels and rotational energy levels were obtained by Raman to determine the crystal composition, and the Raman spectra of the  $\text{Cu}_n\text{Co}_{1-n}\text{-MOF-74}$  can be seen in Figure 2c. The signals of the benzene ring C=C stretching appear around  $1510 \text{ cm}^{-1}$  and  $1620 \text{ cm}^{-1}$ . The strong broad peaks of the samples near  $1570 \text{ cm}^{-1}$  and  $1420 \text{ cm}^{-1}$  can correspond to the asymmetric ( $\nu_{as}$ ) and symmetric ( $\nu_s$ ) modes of the carboxylic acid group  $\text{COO}^-$ , while the strong broad peaks near  $821 \text{ cm}^{-1}$  and  $560 \text{ cm}^{-1}$  correspond to the asymmetric ( $\nu_{as}$ ) and symmetric ( $\nu_s$ ) in-plane deformation mode patterns of the carboxylic acid group  $\beta(\text{COO}^-)$  [13].


 Figure 2 XRD spectrum of  $\text{Cu}_n\text{Co}_{1-n}\text{-MOF-74}$  (a); RAMAN spectrum of  $\text{Cu}_n\text{Co}_{1-n}\text{-MOF-74}$  (b); FTIR spectrum of  $\text{Cu}_n\text{Co}_{1-n}\text{-MOF-74}$  (c); UV spectrum of  $\text{Cu}_n\text{Co}_{1-n}\text{-MOF-74}$  (d).

The morphology of  $\text{Cu}_n\text{Co}_{1-n}\text{-MOF-74}$  was observed using scanning electron microscopy (SEM), and the SEM images showed that all three doping ratios of bimetallic MOF-74 materials have a clear crystal structure (Figure. 3), and the materials exhibit a petal-like structure with the presence of a spherical structure, which is consistent with the morphological description of bimetallic MOF-74 materials in the literature [14]. The semi-quantitative compositional analysis of the sample surface by EDS shows that the distribution of Cu and Co elements is uniform, and the elemental ratios are close to those of the material preparation.


 Figure 3 SEM images of  $\text{Cu}_{0.2}\text{Co}_{0.8}\text{-MOF-74}$  (a); EDS layered images of metal elements in  $\text{Cu}_{0.2}\text{Co}_{0.8}\text{-MOF-74}$  (b); Total spectrum of EDS distribution map of  $\text{Cu}_{0.2}\text{Co}_{0.8}\text{-MOF-74}$  (c); Images of  $\text{Cu}_{0.5}\text{Co}_{0.5}\text{-MOF-74}$  images(d); (e); (f); Images of  $\text{Cu}_{0.8}\text{Co}_{0.2}\text{-MOF-74}$  images(g); (h); (i).

After dissolving the material in a liquid environment for 72 h, the metal ion overflow in the solution was measured, and it could be seen that the metal ion overflow ratio is close to the ion doping ratio of the material itself, and the material is more stable.

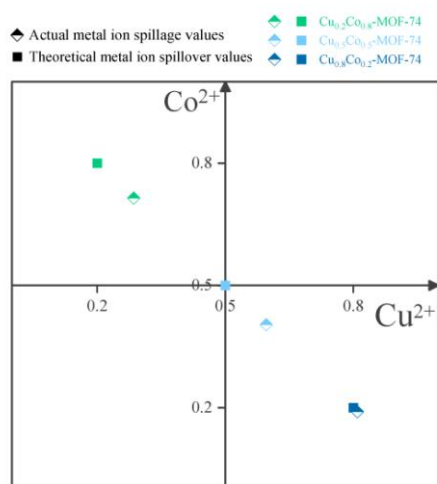


Figure 4 Correspondence diagram of metal ion spillover for  $Cu_nCo_{1-n}$ -MOF-74

#### IV. CONCLUSION

In conclusion, three kinds of  $Cu_nCo_{1-n}$ -MOF-74 materials with different ion doping ratios were successfully prepared. The characteristic peaks in the infrared spectrum of the prepared material are obvious. The crystallinity and crystal structure of the materials are measured by XRD, and the crystal shape of the materials is regular. The distribution of elements on the surface of the material is studied by EDS. It can be found that the two metal elements are evenly distributed on the surface of the material. The stability of the material in water environment was measured by ICP-MS. It was found that the metal ion spillover of the material was close to the ratio of the material preparation. It can be confirmed that the method can synthesize stable  $Cu_nCo_{1-n}$ -MOF-74 with different ion doping ratios.

#### ACKNOWLEDGMENT

We acknowledge financial support from the Fundamental Research Funds for the Central Universities, Southwest Minzu University (No. 2021PTJS36).

#### REFERENCES

[1] Silva, A. R. M., Alexandre, J., Souza, J. E. S., et al. The Chemistry and Applications of Metal-Organic Frameworks (MOFs) as Industrial Enzyme Immobilization Systems [J]. *Molecules*, 2022, 27: 14.  
 [2] Roldan-Carmona, C., Malinkiewicz, O., Soriano, A., et al. Flexible high efficiency perovskite solar cells [J]. *Energ. Environ. Sci.*, 2014, 7(3): 994-997.  
 [3] Wang, Z., Niu, J. S., Zhao, C. Q., et al. A Bimetallic Metal-Organic Framework Encapsulated with DNAzyme for Intracellular Drug Synthesis and Self-Sufficient Gene Therapy [J]. *Angew. Chem. Int. Edit.*, 2021, 60(22): 12431-12437.  
 [4] Geng, Y., Zhang, M. H., Fu, J., et al. MOF-74 and Its Compound: Diverse Synthesis and Broad Application [J]. *Prog. Chem.*, 2021, 33(12): 2283-2308  
 [5] Abedini, H., Shariati, A., Khosravi-Nikou, M. R. Adsorption of propane and propylene on M-MOF-74 (M = Cu, Co): Equilibrium and kinetic study [J]. *Chem. Eng. Res. Des.*, 2020, 153: 96-106  
 [6] Huang, C., Gu, X. Y., Su, X. Y., et al. Controllable synthesis of Co-MOF-74 catalysts and their application in catalytic oxidation of toluene

[J]. *J. Solid. State. Chem.*, 2020, 289: 7.  
 [7] Li, F. F., Chen, Y. N., Gong, M., et al. Core-shell structure Mg-MOF-74@MSiO<sub>2</sub> with mesoporous silica shell having efficiently sustained release ability of magnesium ions potential for bone repair application [J]. *J. Non-Cryst. Solids*, 2023, 600: 10.  
 [8] Chen, T. T., Wang, F. F., Cao, S., et al. In Situ Synthesis of MOF-74 Family for High Areal Energy Density of Aqueous Nickel-Zinc Batteries [J]. *Adv. Mater.*, 2022, 34(30).  
 [9] Chai, L. L., Pan, J. Q., Hu, Y., et al. Rational Design and Growth of MOF-on-MOF Heterostructures [J]. *Small*, 2021, 17(36): 1-31. Wu, T., Liu, X. J., Liu, Y., et al. Application of QD-MOF composites for photocatalysis: Energy production and environmental remediation [J]. *Coordin. Chem. Rev.*, 2019, 403(15): 213097.  
 [10] Gu, X. Y., Huang, C., Xu, Z. C., et al. Core-shell Co-MOF-74@Mn-MOF-74 catalysts with Controllable shell thickness and their enhanced catalytic activity for toluene oxidation [J]. *J. Solid. State. Chem.*, 2021, 294: 121803.  
 [11] Sun, H., Ren, D. N., Kong, R. Q., et al. Tuning 1-hexene/n-hexane adsorption on MOF-74 via constructing Co-Mg bimetallic frameworks [J]. *Micropor. Mesopor. Mat.*, 2019, 284: 151-160  
 [12] Li, C., Qiao, Y. Y., Li, Y. H., et al. Preparation and Application of MOFs/Hydrogel Composites [J]. *Prog. Chem.*, 2021, 33(11): 1964-1971.  
 [13] Strauss, I., Mundstock, A., Hinrichs, D., et al. The Interaction of Guest Molecules with Co-MOF-74: A Vis/NIR and Raman Approach [J]. *Angew. Chem. Int. Edit.*, 2018, 57(25): 7434-7439.  
 [14] Li, H. X., Su, L. Y., Zheng, J. T., et al. MOFs derived carbon supporting CuCo nanospheres as efficient catalysts of peroxymonosulfate for rapid removal of organic pollutant [J]. *Chem. Eng. J.*, 2023, 451: 139114.